



This is a repository copy of *The economics of firm solar power from Li-ion and vanadium flow batteries in California*.

White Rose Research Online URL for this paper:

<https://eprints.whiterose.ac.uk/190540/>

Version: Published Version

Article:

Roberts, D. and Brown, S. orcid.org/0000-0001-8229-8004 (2022) The economics of firm solar power from Li-ion and vanadium flow batteries in California. *MRS Energy & Sustainability*, 9 (2). pp. 129-141. ISSN 2329-2229

<https://doi.org/10.1557/s43581-022-00028-w>

Reuse

This article is distributed under the terms of the Creative Commons Attribution (CC BY) licence. This licence allows you to distribute, remix, tweak, and build upon the work, even commercially, as long as you credit the authors for the original work. More information and the full terms of the licence here:

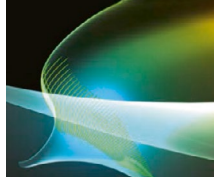
<https://creativecommons.org/licenses/>

Takedown

If you consider content in White Rose Research Online to be in breach of UK law, please notify us by emailing eprints@whiterose.ac.uk including the URL of the record and the reason for the withdrawal request.



eprints@whiterose.ac.uk
<https://eprints.whiterose.ac.uk/>



LARGE-SCALE ENERGY STORAGE - ORIGINAL RESEARCH



The economics of firm solar power from Li-ion and vanadium flow batteries in California

Diarmid Roberts and Solomon Brown , Department of Chemical and Biological Engineering, The University of Sheffield, Mappin St., Sheffield S1 4NL, South Yorkshire, UK

Address all correspondence to Solomon Brown at s.f.brown@sheffield.ac.uk

(Received: 29 November 2021; accepted: 9 May 2021)

ABSTRACT

The cost of providing near 24-7-365 power from solar panels at a commercial facility in South California was modelled to be similar for vanadium flow batteries (VFB) and lithium ion batteries (LIB) at around \$0.20/kWh. In hotter locations, LIB economics suffer due to accelerated background cell ageing. Even within South California there was enough variation to affect the economic comparison. Although LIB degradation could be reduced in a hybrid VFB-LIB system, there was negligible benefit to the overall electricity cost.

As a result of falling photovoltaic panel costs in the last decade solar power (PV) is now claimed to be the cheapest source of electricity. However, the intermittent nature of supply means that it cannot solve the energy trilemma alone, and a form of backup power is required for reliability. This application is well suited to batteries, but the cost implications of providing high levels of reliability in this way have not been widely studied. In this work, the levelised cost of electricity (LCOE) achievable by optimal combinations of PV and batteries is determined for a large food retailer at a range of self-sufficiency ratios (SSR). Both lithium ion batteries (LIB), vanadium redox flow batteries (VFB) and hybrid systems of the two technologies are modelled. In combination with an over-sized PV array, both systems are capable of providing a SSR of 0.95 for a LCOE of less than \$0.22/kWh. The optimal LCOE values overlap across the SSR range for both technologies depending on cost and ambient temperature assumptions. A VFB is more likely to give the lower LCOE at lower SSR, and a LIB is favoured at high SSR as the cycle rate drops as SSR increases. It is also shown that a state of charge (SOC) minimisation strategy has a significant impact on the LIB economics by reducing calendar ageing. Lastly, hybrid systems combining LIB and VFB were modelled, but in no cases showed an improvement over the optimal single choice. The overlap in the LCOE of the two battery types highlights the importance of other considerations, such as sustainability, space requirements and safety.

Keywords energy storage · economics · energy generation · photovoltaic · efficiency · footprint

Discussion

- Although solar power firming superficially appears to be a one cycle per day application, the actual cycle requirement may be much lower, which reduces the value proposition of VFB.
- VFB manufacturers should instead focus their commercial activities in regions with particularly hot climates where LIB background ageing is accelerated.
- Although it may help to reduce capital at risk, vanadium leasing has little effect on the levelised cost of electricity at 5% discount rate.

Introduction

Vanadium flow batteries (VFB) are an interesting class of battery energy storage system (BESS) as the medium, the vanadium electrolyte, has a potentially unlimited lifespan, unlike other BESS. However, they exhibit high costs per unit of power output associated with the electrochemical reactor (stack). This leads to higher capital expenditure (CAPEX) compared to other BESS, such as lithium ion batteries (LIB) at short durations, e.g. 2 h.¹ This has restricted their deployment so far, as the marginal economic return of adding additional duration decreased above 2 h.^{2,3} This is because the reduction in marginal BESS cost is outweighed by the drop in marginal revenue. Additionally, the potential advantage of high cycle life is not realised in the market at present, as BESS are not obliged to cycle every day if the revenue does not justify it.²

Longer storage duration will however be necessary in future grids based upon wind or PV power, as the storage technology is required to take the responsibility for the near 100% reliability currently provided by thermal plant.^{4,5} Depending on the renewable generation mix, the number of cycles the storage must perform each year will vary. In the case of PV, in a market context, the cycling of a BESS would be stimulated by depression of the midday price and/or an increase in the price at other times, particularly the evening when demand is typically highest. Some evidence of this hypothesised price differential is already being seen in domains with high PV penetration.⁶ However, it is not possible to predict what the shape of the price profile will be in future.

Rather than considering the business case of individual BESS projects responding to price signals, there is a class of research that considers the cost of providing a reliable electricity supply at the system level. This could either be at the nationwide electricity grid scale,^{4,5} a subject which has been hotly debated⁷⁻⁹ or a more localised micro-grid scale.^{10,11} The same modelling principles would apply to both cases, although in smaller systems it may be appropriate to model the system at a higher time resolution, as there will be less averaging of renewable power output and demand.⁸ It is not possible to generalise regarding the impact of scale on storage requirements: grids that cover a larger spatial area may be able to achieve greater diversity of renewable generation, but on the other hand, there may be particular micro-grid sites where renewable output is well correlated temporally with local power demand leading to smaller storage needs.

In order to determine the cost of electricity, the total cost of installing and operating the power system may be divided by the total power demand satisfied by generation and storage over the studied period. With the inclusion of a discount rate, this becomes a levelised cost of electricity (LCOE) although various similar terms are commonly used in the literature. This is a more thorough metric than levelised cost of storage (LCOS) which is designed for comparing BESS types and simplifies the generation costs to an assumed price of electricity used to charge the BESS and bases the power demand on an assumed number of storage cycles.^{12,13}

In order to find the lowest cost renewable power supply, optimisation of the BESS should be combined with optimisation of

generation capacity, as over-sizing the latter can be more cost effective than installing storage up to a point.^{4,10} The work of Arbabzadeh et al. is a good example of this¹⁰; starting from a low SSR the cheapest way to increase the SSR is to install greater wind generation capacity. However, at the times of lowest wind output, increasing the capacity to satisfying the demand would be very costly. To further increase the renewable penetration it is then cheaper to install more VFB.

For an electrical grid based on variable renewable power the relationship between LCOE and % of renewable power in the generation mix is non-linear. The gradient of the LCOE versus renewable penetration plot becomes steeper as the latter increases.¹⁴

Given that renewable penetration (as means to CO₂ emissions reduction) and LCOE are both important objectives, a multi-objective optimisation is required to determine the lowest cost configuration of storage and generation across the renewable penetration range.

The above principles also apply to a micro-grid which is aiming to become self-sufficient using storage alongside renewable generation to obtain firm low-carbon power.¹⁰ However, the micro-grid is likely to have a less diverse port.

As the degradation of the BESS will depend on the particular demand profile, renewable generation capacity and BESS power and duration, there is a need to apply accurate degradation models to each instance rather than simply assuming a representative lifetime.

The primary contribution of this work is to perform such multi-objective optimisations for VFB and LIB systems using the most detailed degradation models available for each technology.^{15,16}

The method employed here is to perform a grid search on the variables PV overbuild, BESS power and BESS duration. The first objective is self-sufficiency ratio (SSR) defined as the fraction of total facility load which may be met by the on-site generation.^{17,18} A mixed-integer linear programming approach is used to calculate the SSR that may be achieved by each system.

The second objective is LCOE, as defined in Eq. (18). Once all points are tested, sub-optimal solutions are removed leaving the Pareto set. For any point in this set, it is not possible to reach a higher SSR without increasing the LCOE (or lower LCOE without reducing SSR).¹⁹

The case study is a commercial-industrial facility located in Southern California that is looking to achieve a high SSR using PV and BESS. This is a favourable case study for PV plus BESS economics, as the weather is consistently sunny and the seasonal variation in PV output correlates with the seasonal demand for power, which is likely driven by the need for cooling. As such, it represents a current market in which LIB and VFB would strive to compete.

As temperature is an important factor in LIB degradation a sensitivity study is performed by changing the ambient climate temperature series. The reduction in LIB degradation rate from using a penalty term to minimise SOC when optimising operation is also analysed, as is the impact of changing the assumed CAPEX for each BESS. Lastly, the benefit of a hybrid LIB/VFB system is tested, in which the VFB performs more equivalent full cycles (EFC) than the LIB.

Methods

The case study

This case study is based on a commercial/industrial facility identified as site 281 in a set of 5-min load profile data from 2012.²⁰ It is located in Southern California near lat. 33.62 / long. -116.62 and is classified as ‘‘Grocer/Market’’. The total electrical demand in 2012 was 1583 MWh. The facility is active 7 days a week and displays a broad peak between 6am and 11pm. In the summer, shorter load spikes occur during the active hours, presumably due to air cooling load. Representative days from January to August are shown in Fig. 1.

This building has a floor area of 4543 m², and it is assumed that it is a single storey building, hence has the same roof area. Following²¹ it is assumed that the panel area is 70% of the roof area. Multiplying the panel area by an assumed efficiency of 20% results in a rooftop PV rating of 636 kWp (that is, the output at standard irradiance of 1 kW m⁻²). The output of the PV array was modelled at 36.62° latitude and -116.3° longitude for 2012 using the PVGIS satellite image irradiance model, which predicts actual output at one-hour resolution in W/kWp.²² The slope and azimuth of the panels were assumed to be 10° and 0°, respectively, and it is assumed that there is negligible horizon impingement.

It should be noted that the modelled annual rooftop PV output is 74% of the annual demand; hence, additional PV must be installed on the ground surrounding the building to reach the overbuild ratios considered in the LCOE scenarios.

Round trip AC efficiencies are assumed to be 0.94 and 0.78 for the LIB and VFB, respectively. The derivation of these values is described in S12.

Operational model

The utility of the BESS in supporting self-sufficiency was modelled using a deterministic algebraic modelling approach, whereby the state of the system in each time period is expressed mathematically and a solver is used to optimise the BESS operation. The model was developed by the authors using the Python-based algebraic modelling package PYOMO²³ and passed to the Gurobi solver.²⁴ The operation was optimised 24 h at a time with the assumption of perfect forecasting of PV and demand in this time frame. In the self-sufficiency context it is important that when there is a surplus of PV, the net load is recorded as 0 rather than a negative number. Otherwise the useful output of the PV would be overestimated. It is hence necessary to distinguish between states of power deficit and surplus. This is achieved by including binary indicator variables in the formulation, leading to a mixed-integer linear programming (MILP) problem. The net load at the site at time t is first defined by:

$$\text{minimise} \left(\tau \sum_t P_t^{\text{Imp.}} - \text{SOC}_{\text{final}} \cdot C \cdot \text{Pen.}_{\text{store}} + \text{SOC}_{\text{mean}} \cdot C \cdot \text{Pen.}_{\text{delay-chg}} \right). \quad (6)$$

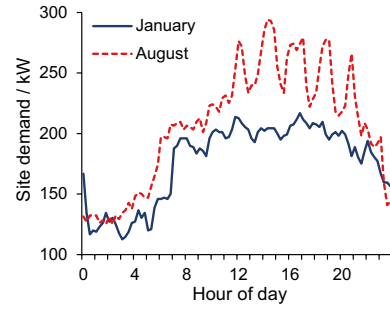


Figure 1. Typical load profiles for winter and summer days at site 281.

$$nl_t = P_t^{\text{Load}} - P_t^{\text{PV}} + c_t - d_t, \quad (1)$$

where P_t^{Load} and P_t^{PV} are exogenous variables representing building load and PV output at time t and c_t and d_t are continuous positive decision variables for BESS charge and discharge (all kW). Energy balance in the BESS is maintained by:

$$\text{SOC}_t = \text{SOC}_{t-1} + \left(c_t \sqrt{\eta_{\text{AC}}} - \frac{d_t}{\sqrt{\eta_{\text{AC}}}} \right) \tau / C, \quad (2)$$

where SOC_t is the fractional state of charge at the end of period t , η_{AC} is the round trip AC energy efficiency (0.94 for LIB, 0.78 for VFB - more detail in S12), τ is the model time step (h, 0.25 in this work) and C is the BESS capacity in kWh. Continuous positive variables for net power import and net power export $P_t^{\text{Imp.}}$ and $P_t^{\text{Exp.}}$ (kW) are next introduced and used to distinguish between the cases where $nl_t > 0$ and the cases where $nl_t < 0$. For example, if $nl_t > 0$, $P_t^{\text{Imp.}}$ is set to nl_t and $P_t^{\text{Exp.}}$ is set to 0. This, the export case and the case of neither export nor import are enforced by:

$$nl_t = P_t^{\text{Imp.}} - P_t^{\text{Exp.}} \quad (3)$$

$$P_t^{\text{Exp.}} - M(\delta_t^{\text{Exp.}}) \leq 0 \quad (4)$$

$$P_t^{\text{Imp.}} - M(1 - \delta_t^{\text{Exp.}}) \leq 0 \quad (5)$$

where $\delta_t^{\text{Exp.}}$ is a binary indicator variable which takes the value 1 for export and M is an arbitrarily large constant*. Additional constraints are posed keeping SOC_t between 0 and 1 and keeping c_t and d_t equal to or less than the rated power of the BESS.

The objective of maximising self-sufficiency is identical to minimising imports and is hence defined by:

* Note: Care must be taken when setting M in this case study, as it must be larger than the possible import or export across all PV array sizes and load profiles studied otherwise there may not be a feasible solution.

The second and third terms in the objective are expressions (kWh) for controlling SOC. The first of these ensures that if there is an overall surplus of PV in the optimisation window, the BESS stores it for use in the next window. The penalty term $\text{Pen}_{\text{store}}$ was set at 0.1 so that this objective is always subordinate to the primary objective of minimising imports in the current window. The second penalty minimises SOC_{mean} the average SOC, which in LIB systems reduces calendar ageing (Eq. 10). The penalty $\text{Pen}_{\text{delay-chg}}$ was set to 0.01, so that this delaying of charging is subordinate to both the other objectives, i.e. it only occurs if imports are minimised and there is flexibility in when to charge whilst still maximising the SOC carried into the next period. SOC does not influence VFB degradation in the degradation model applied in this work, so $\text{Pen}_{\text{delay}}$ is set to 0.

The SSR is subsequently calculated by:

$$SSR = 1 - \frac{\tau \sum_t P_t^{\text{Imp.}} + E_{\text{rebalance}}}{\tau \sum_t P_t^{\text{Load}}}, \quad (7)$$

$$\beta_{\text{cap}} = 7.348 \cdot 10^{-3} \cdot (\bar{V} - 3.667)^2 + 7.600 \cdot 10^{-4} + 4.081 \cdot 10^{-3} \cdot \Delta\text{DOD}, \quad (12)$$

where $E_{\text{rebalance}}$ is the energy required to continually rebalance the VFB across the period as defined in Eq. (17) (set to 0 for LIB).

Hybrid model

For the hybrid LIB / VRFB system charge and discharge variables are defined for both components, and Eqs. (1) and (2) redefined accordingly. The objective is defined by:

$$\text{minimise} \left(\tau \sum_t P_t^{\text{Imp.}} + \text{Pen}_{\text{priority}} \tau \sum_t d_{\text{LIB},t} - (\text{SOC}_{\text{final,LIB}} + \text{SOC}_{\text{final,VRFB}}) C \cdot \text{Pen}_{\text{Fill}} + \text{SOC}_{\text{mean, LIB}} C \cdot \text{Pen}_{\text{Delay}} \right). \quad (8)$$

By setting $\text{Pen}_{\text{priority}}$ to 0.8, the penalty was larger than the loss in self-sufficiency due to the lower round trip efficiency of the VFB, but not large enough to prevent the LIB cycling if the VFB is full.

Degradation models

The PV rating (kWp) is assumed to degrade at a rate of 0.5% per year, based on the analysis in Ref. [25].

For both LIB and VFB, the degradation is calculated at the end of the each period of simulation by applying a rainflow-counting algorithm to the SOC profile.²⁶ This function breaks the SOC profile into sets of whole and half cycles and returns the depth of discharge and average SOC for each element in each set. More detail on the models employed is given in the following subsections.

LIB

The LIB degradation is calculated daily using the model reported by Schmalstieg et al.¹⁶ who defined the capacity of the battery relative to the initial value as:

$$C = 1 - \alpha_{\text{cap}} \cdot d^{0.75} - \beta_{\text{cap}} \cdot \sqrt{Q}. \quad (9)$$

In the first term, describing calendar ageing, d is the time in days since the start of service and α_{cap} is the calendar ageing factor. The second term describes the cycle ageing in terms of equivalent full cycles (EFC) Q and the cycle ageing factor β_{cap} . α_{cap} is defined by:

$$\alpha_{\text{cap}} = (7.543V - 23.75) \cdot 10^6 \cdot e^{-6976/T}, \quad (10)$$

where T is the cell temperature (K) and V is the cell voltage approximated by:

$$V = a \cdot \text{SOC} + b, \quad (11)$$

where a and b are empirically derived parameters.

β_{cap} is defined by:

where \bar{V} is the mean cell voltage across the cycle and ΔDOD the depth of discharge.

For the purposes of the present work, where it is necessary to calculate the degradation following each implemented schedule, it is necessary to take the derivatives of the calendar and cycle ageing expressions. The derivative of the calendar ageing expression with respect to time and the derivative of the cycle

ageing expression with respect to cycles are defined, respectively, by:

$$\frac{dC}{dd} = -0.75 \cdot \alpha_{\text{cap}} \cdot d^{-0.25} \quad (13)$$

and

$$\frac{dC}{dQ} = -0.5 \cdot \beta_{\text{cap}} \cdot Q^{-0.5}. \quad (14)$$

It is assumed that the length of the optimisation period and the energy throughput are sufficiently small relative to the project history, so that the change in gradient across the schedule may be ignored. It is also assumed that because the average cell voltage does not change with time, the coulombic expression

of Schmalstieg et al. (A h) may be directly converted to energy (kWh). Lastly, as in Schmalstieg et al., it is assumed that cycle ageing and calendar ageing are independent processes. The absolute degradation in a schedule beginning at d days, where W whole cycles and H half cycles are performed, may hence be defined by:

$$\Delta C = C_0 \cdot \left(0.75\tau \cdot \sum_t \alpha_{\text{cap}_t} \cdot d^{-0.25} \cdot + 0.5 \cdot Q^{-0.5} \left(\sum_w \beta_{C,w} \cdot \Delta DOD_w + \sum_h \beta_{C,h} \cdot 0.5 \cdot \Delta DOD_h \right) \right), \quad (15)$$

where C_0 is the starting capacity of the LIB in kWh. The calendar ageing was calculated in each model period t using hourly temperature data obtained from weather stations in Southern California and assuming that the cell temperature is equal to the ambient temperature (see SI3).

It is assumed that the LIB will be replaced when the capacity reaches 80% of the original. The corresponding increase to internal resistance reported by¹⁶ was not modelled. This is not expected to impact the results in a meaningful way, as the LIB starts with a very low resistance (see SI2) and the C-rates studied in this work are low due to multi-hour duration of systems.

VFB

For the VFB, a model recently published by Rodby et al. is applied, which considers both the loss of capacity due to vanadium crossover (“capacity fade”) and oxidation state drift due to side reactions (“electrolyte decay”).¹⁵

Both of these processes are reversible. For capacity fade it is assumed that the rebalancing process is continual. Hence the working capacity is not affected, but the energy required to rebalance the electrolyte is subtracted from the energy delivered by the VFB in the LCOE calculation. This is a conservative assumption—in practice the energy required to rebalance the system will often be free, due to PV over-sizing.

It is first assumed as in¹⁵ that a fade of $f\%$ is due to $f\%$ of the vanadium in the anolyte (average oxidation state 2.5) crossing the membrane and reacting with $f\%$ of the catholyte (average oxidation state 4.5) to give $2f$ vanadium with an oxidation state of 3.5. The resultant deficit in the oxidation state of the catholyte in the discharged state is hence defined by:

$$\delta_{\text{catholyte}}^{\text{Ox}} = 4 - \frac{2f \cdot 3.5 + (100 - f) \cdot 4}{100 + f}. \quad (16)$$

Because the redox reaction in the VFB involves the transfer of one electron, the energy (kWh) required to rebalance the system may be calculated by:

$$E_{\text{rebalance}} = \frac{C \delta_{\text{catholyte}}^{\text{Ox}}}{\sqrt{\eta_{AC}}} (1 - f_{ED}). \quad (17)$$

As in Rodby et al. the maximum capacity is reduced by f_{ED} , the cumulative electrolyte decay since the last maintenance visit, and the fade rate f is set at 0.66% per cycle.¹⁵

For electrolyte decay, the rate of 0.09% per cycle reported by Rodby *et al.* is multiplied by the number of EFC performed in the scheduled period. In this case study, the average working capacity of the VFB across the year was typically 0.89 of the nameplate capacity as a result of electrolyte decay. The maintenance is scheduled for May, although this timing has not been

optimised. It is assumed that the maintenance intervention will be performed annually at the time of general maintenance and hence incur negligible additional costs.

Stack degradation is accounted for by pricing in a replacement stack halfway through the project after.²⁷

Economic model

CAPEX

Both technologies are priced based on the accessible depth of discharge (DoD) such that a 4-h system has a genuine 4-h capacity (excluding losses). For the LIB the DoD is set at 0.8 (SOC 0.1–0.9) after¹ and for the VFB it is set at 0.7 (0.15–0.85) after.²⁸

Estimates of 2020 and 2030 prices for LIB modules with NMC electrodes are taken from a 2020 report by PNNL.¹ As the project is assumed to start in 2025, the prices were interpolated, giving \$155/kWh for the base scenario (PNNL mid-price case). As the PNNL price estimates are based on a 100% DoD, this value is scaled to \$194/kWh based on the accessible DoD of 0.8.

The price of the VFB at the DC boundary was calculated using a bottom-up model, based on the performance parameters of a kW scale system reported by Ref. [28]. The model is defined in SI1. In the base scenario, the DC module price is calculated from the obtained power and energy specific prices of \$283/kW and \$145/kWh, respectively. The latter price is based on the average vanadium pentoxide price of \$17/kg from January 2006 to April 2020.²⁹

For both BESS, the balance of costs required for a turnkey AC system (BTC) is estimated using the model described in Ref. [30]. The lower energy density of the VFB is accounted for by multiplying the engineering, procurement and construction (EPC) costs by a “footprint” factor of 1.7 to reflect the higher cost associated with preparing a larger site (after^{30,31}).

The first 640 kWp of PV is assumed to be installed on the roof (“The Case Study” section), at a cost of \$1650 per kWp, achieved by removing the inverter field from the 2020 price reported for commercial rooftop PV by NREL.³² Additional PV is assumed to be ground mounted and cost \$1280 per kWp, which is midway between the rooftop value and the utility scale fixed mount cost of \$900 per kWp (excluding inverter) from the same source. To the total cost is applied the investment tax credit (ITC), which, for projects installed after 2023, will give a 10% rebate on PV installations.³³

Table 1. Additional cash flow items for LIB and VRFB during the 20-year project.

Year	BESS	Item	Cost
Variable	LIB	DC module replacement	\$145 to \$194/kWh
10	LIB/VFB	Inverter replacement	\$205/kW
10	VFB	Stack replacement	\$283/kW
20	LIB	DC module recovery	− \$145/kWh ^a
20	VFB	Electrolyte recovery	− \$142/kWh

Negative cost represents income.

^aThe replacement cost of LIB modules depends on the replacement year. Between 2025 and 2030, the price is interpolated, and after 2030 it is held constant. The residual value is then adjusted pro-rata to the fraction of life remaining relative to the 0.8 SoH end of life definition. Prices shown are for the mid-price scenario.

In this work, the inverter cost is likely overestimated, as the power rating is specified to match the rated output of the BESS. In practice, the highest power is during charging of the BESS from PV, which could be done via a DC bus, so a smaller inverter could be specified.

OPEX

The operation and maintenance costs (O&M) associated with the PV array is priced at \$19/kW after.³² The O&M associated with both BESS types is priced at \$10/kW after.^{31,34} This estimate does not include augmentation, as the degradation is dealt with elsewhere in the model (see “[Degradation Models](#)” section). The O&M costs are assumed to increase by 2% per year from the project start in 2025.

Other cash flows

Other costs and incomes associated with equipment replacement and recovery are given in Table 1.

Levelised cost of electricity calculation

The levelised cost of electricity in \$/kWh is calculated by:

$$LCOE = \frac{CAPEX + \sum_n \frac{O\&M_n + Other_n}{(1+i)^n}}{\sum_n \frac{E_{supplied,n}}{(1+i)^n}}, \quad (18)$$

where n is the project year and i is the fractional discount rate, which is set at 5% after.³² $E_{supplied,n}$ (kWh) is the electricity supplied by the PV and BESS to the site, defined by:

$$E_{supplied,n} = \tau \sum_t \left(P_{n,t}^{Load} - \max(nI_{n,t}, 0) \right) - E_{rebalance,n}. \quad (19)$$

For the LIB, the rebalance cost in Eq. (19) is set to 0.

Results and discussion

CAPEX of Turnkey BESS

For the base scenario, the modelled CAPEX required for turnkey LIB and VFB systems at a range of durations are shown in Figs. 2 and 3.

In the BTC model EPC costs scale primarily with energy rating, whereas the balance of system hardware (BOSH) costs scale primarily with power rating. Hence EPC costs make up an increasing proportion of the system price as duration increases.

The data in Figs. 2 and 3 show that the VFB is predicted to be 29% more expensive than the LIB at 2-h duration, 14% more expensive at 4-h duration and then approach the LIB price as duration increases further. Although the VFB is cheaper on a DC \$/kWh basis by 6-h duration, the higher EPC costs predicted in the model by the 1.7 footprint factor push the turnkey price higher. Recent PNNL estimates for CAPEX give a slightly larger difference between VFB and LIB CAPEX than that shown in Figs. 2 and 3, although this is partly due to the accessible DoD of 0.8 for the LIB not being factored at the pricing stage.¹ For this reason, the higher power cost scenario for the VFB is included in “[Sensitivity Study on Economic and Environmental Factors](#)” section.

LCOE versus self-sufficiency ratio for each BESS

Approximate Pareto fronts for minimisation of LCOE and maximisation of SSR were obtained manually by removing sub-optimal points from the dataset obtained from the grid search in PV:Load ratio, BESS power rating and BESS duration. PV:Load ratio is the ratio of total annual modelled PV output to total annual load. The LIB front is shown in Fig. 4 and the VFB front in Fig. 5.

The Pareto fronts display an inflexion point around 0.9 SSR for both technologies. Depending on the cost of alternative electricity sources (e.g. imports or on-site generation, such as a natural gas or diesel gensets) this would be a candidate for optimal

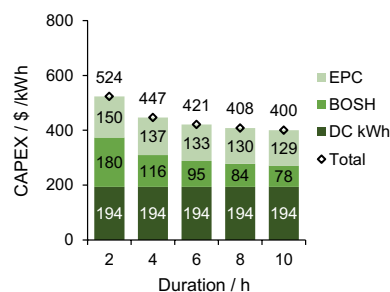


Figure 2. Turnkey price breakdown for LIB systems specified with a range of durations. The LIB module price is the mid case.

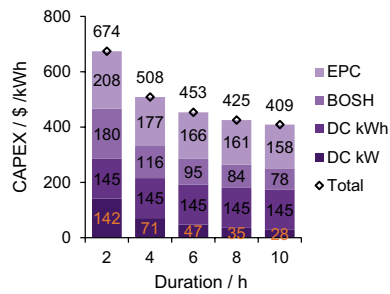


Figure 3. Turnkey price breakdown for VFB systems specified with a range of durations.

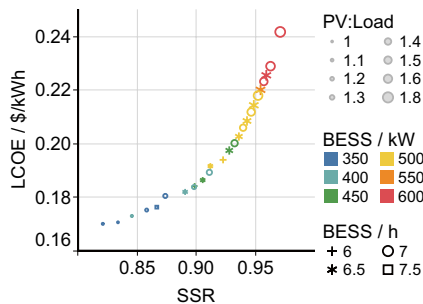


Figure 4. Approximate Pareto front for maximisation of SSR and minimisation of LCOE with PV and LIB of varying ratings.

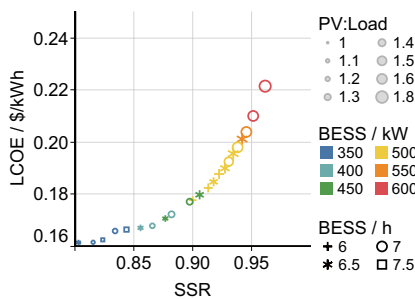


Figure 5. Approximate Pareto front for maximisation of SSR and minimisation of LCOE with PV and VFB of varying ratings.

sizing, as additional over-sizing brings diminishing returns. The optimal duration is 7–7.5 h at lower SSR and decreases slightly to 6.5–7 h at higher SSR. This is because the over-sizing of the PV array for high SSR reduces the daily hours of deficit which must be covered.

At a given SSR target, the required VFB capacity is greater than the required LIB capacity. For example, at 0.95 SSR, the optimal VFB specification is 600 kW/7 h, whereas the optimal LIB specification is 500 kW and between 6.5 and 7 h. This is due to the effective capacity of the VFB being lower because of its lower efficiency. However, the installed PV capacity is the same in both cases, at 160% over-sizing. This is because the PV over-sizing is dictated primarily by the seasonal variation.

Despite the greater VFB capacity requirement, in the base scenario, the VFB gives a lower LCOE than the LIB, and the gap is consistent across the SSR range at approximately $\text{€}0.7/\text{kWh}$. This consistency is surprising, as the EFC performed by the LIB should be lower at high SSR, as increasing the battery size to meet SSR requirements will lead to it being cycled less deeply on average. Indeed the 400 kW/6.5 h LIB that delivers 0.89 SSR performs 0.67 EFC per day, whereas the 600 kW/6.5 h LIB that delivers 0.96 SSR performs 0.50 EFC per day. This leads to an increase in the LIB lifetime, as shown in the “MARB” scenarios in Fig. 6.

However, the lifetime is not a simple reciprocal of the cycle rate and the high SSR system only lasts 18% longer than the low SSR system (8 years and 4 months vs. 7 years and 1 month) compared to 34% as implied by the cycle rate alone. The reason for the relatively poor lifetime of the LIB at high SSR is analysed in “[Extending LIB lifetime by SOC minimisation](#)” section. Figure 6 also shows that the working capacity of the VFB is also increased at high SSR, due to the lower cycle count which results in lower electrolyte decay. Despite the apparently flat capacity profile, the VFB working capacity actually oscillates between the values shown at year end in Fig. 6 and a low end value of 0.80, which maintenance is timed to coincide with.

Sensitivity study on economic and environmental factors

In this section, the impact of changing several economic parameters is investigated, in order to gauge the robustness of the results. The LIB DC module price was reduced to the low end projection made by Ref. 1] (see “CAPEX” section), and the ambient temperature was reduced by simulating the San Diego site and then by subtracting 2K from that temperature series. On the VFB side, electrolyte leasing and EPC reductions were both tested. A high power price case was also modelled, in which only half of the projected reduction in power specific costs by 2025 is achieved, giving a DC price of $\text{\$}389/\text{kW}$ for both the initial CAPEX and the year ten replacement.

Approximate Pareto fronts for the various cases are shown in Fig. 7.

On the LIB side of the comparison, the future price of the DC modules is the dominant factor. Under the mid-price projection, the LIB LCOE is greater than or equal to the base VFB LCOE at all points on the front in all temperature scenarios. Under the low price assumption, the LIB LCOE is equal to or less than the base VFB LCOE under all temperature assumptions.

Temperature has an important impact on LIB lifetime as shown in Fig. 6 (but no effect on VFB lifetime in the degradation model applied here¹⁵). LIB at the San Diego location are predicted to last 1 year longer than those at the MARB location in the low SSR case and almost 2 years longer in the high SSR case. The reduction from the March Air Reserve Base site to the San Diego site with the -2K offset reducing the LCOE by approximately $\text{€}0.5/\text{kWh}$ at 0.82 SSR and $\text{€}0.7/\text{kWh}$ at higher SSR. The drop is greater at high SSR both because the life extension is greater (as shown in Fig. 6) and because the LIB modules comprise a higher proportion of the overall project costs. Further

Figure 6. Degradation profiles showing year end SoH for both LIB and VFB at high and low SSR. For the LIB, “MARB” denotes the March Air Reserve Base site (base scenario) and “SD” the more temperate San Diego International Airport site.

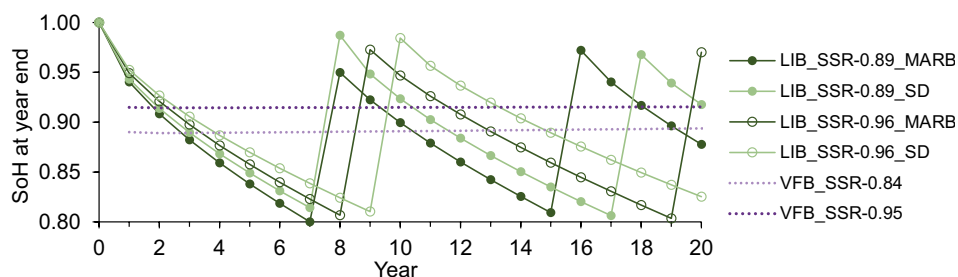
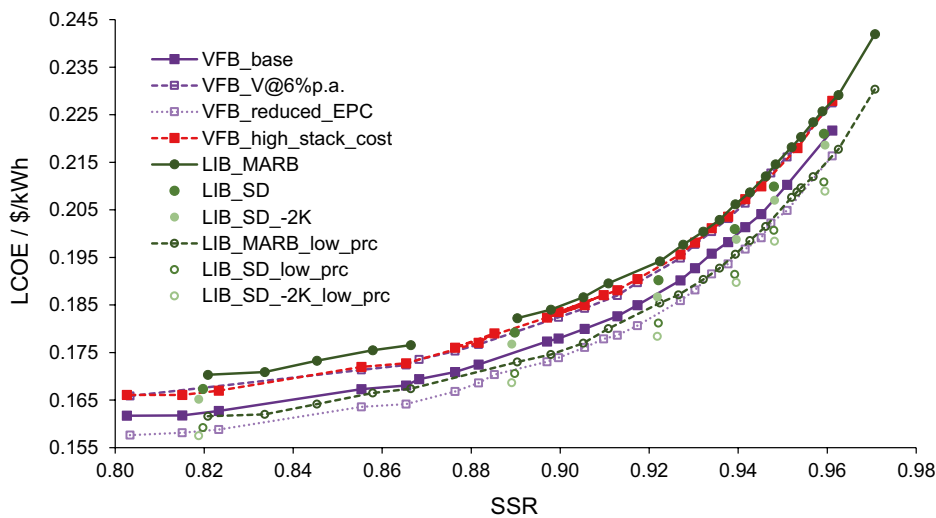


Figure 7. Pareto fronts for VFB and LIB under various scenarios. For VFB, “V@6%p.a.” denotes electrolyte leasing, and “reduced EPC” is due to a reduction in assumed system footprint from 1.7 x LIB footprint to 1.2 x LIB. For the LIB, “MARB” denotes the March Air Reserve Base site (base scenario) and “SD” the more temperate San Diego International Airport site. “low_prc” indicates the low price projection as opposed to the mid-price projection in the base scenario (see “CAPEX” section).



reductions in ambient temperature will show decreasing impact due to the Arrhenius-type behaviour reported by Schmalstieg et al.¹⁶ At low SSR, reducing the temperature reduces the modelled SSR slightly, which is counter intuitive as degradation is slower. This is due to the non-linear nature of degradation; as the degradation slows, the LIB spends more of the project at a reduced working capacity. This effect is not as strong at high SSR, as the lifetime is longer due to reduced cycle rate. Hence the slower drop in working capacity due to temperature reduction dominates.

On the VFB side, leasing the electrolyte at 6% actually has a negative impact on LCOE. This is because the discount rate is 5% and the project life is 20 years; hence, the total discounted lease payment is higher than the CAPEX minus the recovered electrolyte value in the base case.

Reducing the footprint factor from the 1.7 average from^{31,35} to 1.2 reduces the LCOE by about $\text{\textsterling}0.4$ /kWh. In a more recent cost comparison, PNNL reported the EPC costs for LIB and VFB systems as being approximately the same, so the lower figure may be more appropriate.¹

In the high stack cost case, the VFB front goes from being roughly equivalent to the low price LIB front, to being roughly equivalent to the mid-price LIB front.

Overall, the economics of self-sufficiency of the LIB and VFB are quite similar, and the distributions of Pareto fronts overlap.

Extending LIB lifetime by SOC minimisation

The experimental work of Schmalstieg et al. showed that background ageing is accelerated at high SOC.¹⁶

In this section the impact of such a strategy on the self-sufficiency economics of LIB systems is studied. Where a PV surplus exists, the penalty term *Pen.Fill* in Eq. (6) ensures that the LIB will store as much of this surplus as possible, but as late as possible. By extending the optimisation window to 48 h, it will not store more than necessary on the first day if there will be a surplus on the next day too. As only the first 24 h of this schedule is implemented, on consecutive days with PV surplus, the LIB will not spend time at a higher SOC than necessary.

The impact of the SOC consideration is greatest in the summer months, as shown in Fig. 8.

In summer the high PV output leads to a smaller residual load, and the cycle rate required of the BESS is smaller. When the optimisation window is 24 h the LIB fills with surplus PV and rarely discharges fully. Extending the optimisation window to 48 h and applying the penalty on average SOC forces the LIB to only store what it requires to cover any shortfall the following day. This reduces the average SOC across the first year of operation from 0.45 to 0.39 and increases the lifetime from 6 years and 9 months to 7 years and 1 month. The impact is greater for the larger LIBs specified to provide higher SSR. In these cases the LIB is cycled less, and without a SOC minimisation strategy, sits idle at a high SOC for a greater fraction of the time. For the

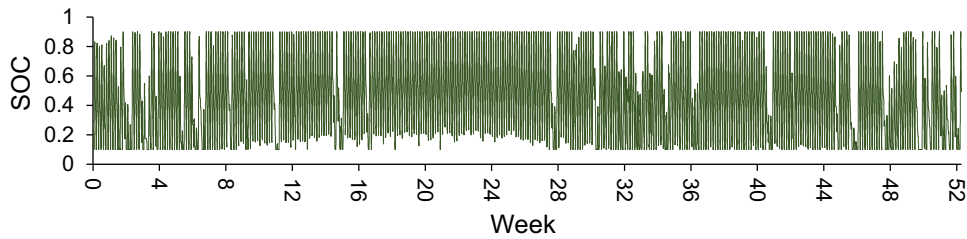


Figure 8. SOC profile of a 1080-kW/6-h LIB across 1 year of operation providing self-sufficiency at site 281 when paired with a 1080 kWp PV array (120% over-sizing). Consistent PV surplus in the summer leads to an elevated SOC.

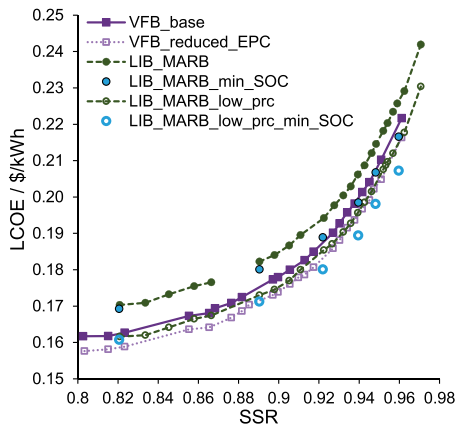
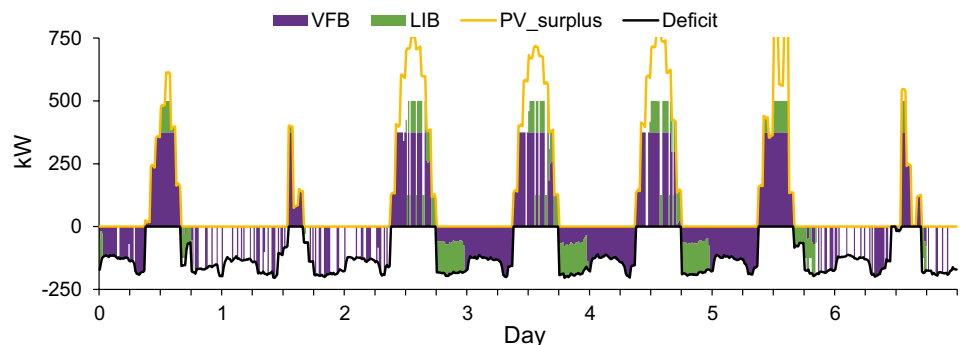


Figure 9. The Pareto fronts for LIB installations with and without SOC minimisation strategy, compared to other cases. For VFB “reduced EPC” denotes a reduction in assumed system footprint from 1.7 x LIB footprint to 1.2 x LIB. For the LIB, “MARB” denotes the March Air Reserve Base site (base scenario), and “low_prc” indicates the low price projection as opposed to the mid-price projection in the base scenario (see CAPEX section).

600 kW/6.5 h LIB paired with the 1440 kWp PV array, the SOC penalty reduces the mean SOC from 0.57 to 0.33, extending the lifetime from 8 years and 6 months to 11 years and 9 months.

Several points on the LIB Pareto front shown in Fig. 7 are re-run using the 48-h optimisation with the SOC penalty. Figure 9 shows how the LCOE falls at various points on the Pareto front.

Figure 10. A snapshot of the optimal dispatch at site 281 during February of a hybrid BESS consisting of a 375-kW/6-h VFB and a 125-kW/6-h LIB paired with a 1350 kWp PV array.



The decrease in LCOE is greatest at higher SSR for the reasons outlined above. Overall the SOC minimisation strategy does not result in a meaningful change to the VFB / LIB comparison at low SSR, but at high SSR it can reduce the LCOE by £0.8 /kWh pushing the balance in favour of the LIB.

It is important to note that since the SOC minimisation strategy relies on forecasting, it will be better suited to some sites than others. At site 281 the total demand varies little from one day to the next, but at sites with more variability the approach of storing just enough electricity to cover the predicted demand would carry greater risk.

Evaluating the benefit of hybrid LIB/VFB systems

Using both technologies in a hybrid system it should be possible to perform the daily cycling with a suitably sized VFB and the less frequent cycling for days of higher net load with an LIB. Site 281 is active 7 days a week, and hence the variability in the load profile comes primarily from PV output fluctuations, with summer days giving longer hours of net PV surplus.

In this section the results of an MILP co-optimisation of several VFB:LIB hybrid combinations are compared to the individual systems. A snapshot of the optimal schedule for the 75:25 VFB:LIB hybrid at the 500-kW/6-h specification is shown in Figs. 10 and 11.

The hybrid schedule optimisation is successful in that the VFB is charged preferentially. If the LIB must be charged, this is done as late as possible, and once the system moves to a power deficit the LIB discharges first.

Figure 11. SOC profiles of LIB and VFB corresponding to the dispatch shown in Fig. 10.

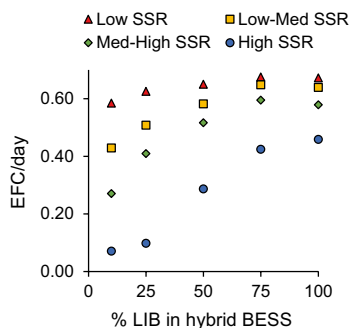
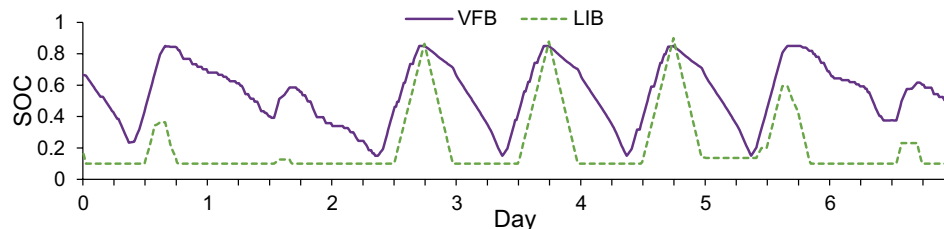


Figure 12. The variation in LIB equivalent full cycle rate due to varying the fraction of the hybrid BESS it comprises. Results are shown for four PV:BESS specifications corresponding to a range of SSR values.

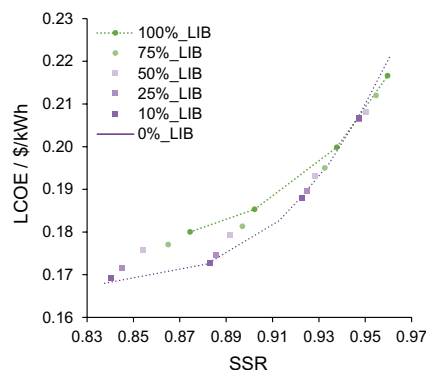


Figure 14. A comparison of the economics of hybrid VFB:LIB systems with those of the optimal single BESS systems. 0% LIB indicates a 100% VFB system.

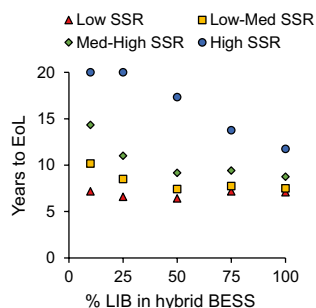


Figure 13. The variation in LIB lifetime (to 0.8 state of health) due to varying the fraction of the hybrid BESS it comprises. Results are shown for four PV:BESS specifications corresponding to a range of SSR values.

The impacts of the hybridisation on the cycle rate and lifetime of the LIB component are shown in Figs. 12 and 13. It is interesting to note that in the high SSR case, the 100% LIB system performs only 0.46 EFC/day. This is very different to the intuitive notion that providing PV firm power would require one cycle per day. The data show that hybridisation has the expected effect of reducing the LIB cycle rate and extends the lifetime. The lifetime extension is greatest at high SSR, where the overall system is over-sized, hence the VFB can cover a higher proportion of the overall duty.

Generating a full Pareto front in SSR and LCOE for the hybrid system is out with the scope of this work, as adding two new dimensions, LIB:VFB power ratio and LIB:VFB duration ratio would greatly increase the computation and data processing

time. Hybridisation was hence evaluated at four points: PV 1080 kW_p / BESS: 400 kW/6 h, PV 1170 kW_p / BESS: 400 kW/6.5 h–7 h, PV: 1350 kW_p / BESS: 500 kW/6 h, and PV: 1440 kW_p / BESS: 600 kW/6.5 h.

These points were chosen as they lie on the Pareto front for both BESS types (except the 1170 kW_p point, in which case the duration was set at 6.5 h for the LIB and 7 h for the VFB). The ratio of the VFB power rating to LIB power rating (assuming each has its own inverter) was varied at each point, and the resultant LCOE versus SSR data are shown in Fig. 14.

The results in Fig. 14 show that there is no economic benefit to deploying a hybrid system, as at each SSR point the hybrid systems simply follow a trend between the pure VFB and pure LIB points and do not move outside of the two Pareto fronts. This is somewhat surprising given the increases to LIB lifetime seen in the hybrid cases. However, it is important to note the trade-offs. As the LIB size is reduced, the lifetime is extended, but this has less weighting in the overall economic outcome.

Conclusion

The analysis performed in this work shows that for a commercial/industrial facility in Southern California, self-sufficiency ratios of 0.95 and above may be reached whilst achieving a LCOE of \$0.22/kWh or below. Between 0.8 and 0.95 SSR, the optimum duration of both systems is 6–7.5 h. The optimal choice of LIB or VFB depends on both the CAPEX assumptions and the

assumptions regarding LIB cell temperature with respect to the ambient climate.

The LIB is more likely to be the cheaper option at high SSR, as the required battery over-sizing results in a reduced cycle count. VFB manufacturers should focus on sites with high upper ambient temperature ranges, as LIB will suffer increased LCOE in these situations.

The ability to predict site load is important for preserving the lifetime of the LIB. When the load is predictable, deploying the LIB to only store enough PV output allows the average SOC to be reduced, which considerably improves the LCOE at high SSR.

Whilst a hybrid LIB/VFB system (equivalent duration, differing power rating) is shown to result in extension of LIB lifetime by giving cycle priority to the VFB, no benefit to such a system is found at the LCOE level. This is attributed to the countering of the improved lifetime by the reduced contribution of the LIB.

The Pareto front for LCOE versus SSR steepens at 0.9 for both BESS types, and this may hence be an optimum for system sizing. However, this will depend on the cost of the options available for dealing with the remaining deficit. For example, the remaining deficit could be covered by either diesel or natural gas micro-generation or triaged according to priority. Further work on such optimisation would benefit from load data that is decomposed with individual sub-loads assigned priorities.

Given the overlap in LCOE for LIB and VFB depending on the scenario, it is likely that other factors will come into consideration when making the choice between the two technologies. For example, the achievable energy density of the VFB and LIB including all balance of plant may be a deciding factor if space is at a premium. Alternatively, the reduced fire risk of the VFB could be a deciding factor. Sustainability metrics relating to the resources required in their manufacture and disposal are also becoming increasingly important. Further work is required to quantify these factors.

Given the advantages of lithium-iron phosphate (LFP) batteries, namely cheaper materials and longer cycle life, it is quite possible that this technology will be the real competitor for VFB in the near term rather than the NMC batteries modelled in this work.¹ Extending the study to LFP batteries would hence be informative for the business case for VFB. Even within the NMC chemistry, it is likely that improvements since 2014 will have reduced the degradation rate. There is also considerable uncertainty regarding the actual temperature within the cells contained in a pack, when compared to experiments carried out on single cells. On one side, thermal inertia may prevent the cells from reaching the peak ambient temperature, which would reduce calendar ageing. On the other side, heat generated during operation may lead to higher temperatures within the module, as even C-rates of 1/5 lead to several degrees of warming at the single cell level.³⁶ A further level of optimisation may be required to study the trade-off between actively cooling the modules to prolong life and the CAPEX and OPEX associated with such cooling.

Although it is shown that pushing down the average SOC can increase lifetime considerably, there is scope for further improvement. In the model described by Schmalstieg et al.,

a micro-cycle centred at a high or low SOC is more damaging than one centred at 0.5 SOC.¹⁶ The optimal schedule may hence involve a slightly higher SOC than the one obtained by the methods reported here. This would also have the benefit of reducing risk of premature draining due to forecasting uncertainty. More advanced cycle depth optimisation methods have been reported elsewhere, but not for MILP optimisation problems, such as the self-sufficiency maximisation.³⁷

Lastly, there is uncertainty regarding the necessary replacement point of LIB. Beyond a certain point, the degradation of an NMC cathode accelerates due to capacity imbalance caused by progressive capacity loss in the anode.³⁸ Although 0.8 SoH has been used as an end of life point by other researchers,² this may be overly conservative and inspired by EV applications.

Acknowledgments

This work was supported by the UK Engineering and Physical Science Research Council via grant EP/L016818/1 which funds the Centre for Doctoral Training in Energy Storage and its Applications. The authors are also grateful to Drax Power Ltd. for their financial support.

Data availability

The datasets generated during and/or analysed during the current study are available in the GitHub repository, https://github.com/diarmidr/PV_plus_storage_LCOE_v_SSR.

Declarations

Conflict of interests The authors have no competing interests to declare.

Supplementary Information

The online version contains supplementary material available at <https://doi.org/10.1557/s43581-022-00028-w>.

Open Access

This article is licensed under a Creative Commons Attribution 4.0 International License, which permits use, sharing, adaptation, distribution and reproduction in any medium or format, as long as you give appropriate credit to the original author(s) and the source, provide a link to the Creative Commons licence, and indicate if changes were made. The images or other third party material in this article are included in the article's Creative Commons licence, unless indicated otherwise in a credit line to the material. If material is not included in the article's Creative Commons licence and your intended use is not permitted by statutory regulation or exceeds the permitted use, you will need to obtain permission directly from the copyright holder. To view a copy of this licence, visit <http://creativecommons.org/licenses/by/4.0/>.

REFERENCES

1. K. Mongird, V. Viswanathan, J. Alam, C. Vartarian, V. Sprenkle, *2020 Grid Energy Storage Technology Cost and Performance Assessment*. Technical report, PNNL (2020)
2. M. Fisher, J. Apt, J.F. Whitacre, Can flow batteries scale in the behind-the-meter commercial and industrial market? A techno-economic comparison of storage technologies in California. *J. Power Sources* **420**, 1–8 (2019). <https://doi.org/10.1016/J.JPOWSOUR.2019.02.051>
3. C. Crespo Montañés, W. Gorman, A.D. Mills, J. Hyungkwan Kim, Keep it short: exploring the impacts of configuration choices on the recent economics of solar-plus-battery and wind-plus-battery hybrid energy plants (2021). https://eta-publications.lbl.gov/sites/default/files/doi_webinar_hybrid_configuration_briefing_final.pdf. Accessed 24 Nov 2021
4. B. Cárdenas, L. Swinfen-Styles, J. Rouse, A. Hoskin, W. Xu, S.D. Garvey, Energy storage capacity vs. renewable penetration: a study for the UK. *Renew. Energy* **171**, 849–867 (2021). <https://doi.org/10.1016/j.renene.2021.02.149>
5. M.Z. Jacobson, M.A. Delucchi, M.A. Cameron, B.A. Frew, Low-cost solution to the grid reliability problem with 100% penetration of intermittent wind, water, and solar for all purposes. *Proc. Natl. Acad. Sci. USA* **112**(49), 15060–15065 (2015). <https://doi.org/10.1073/PNAS.1510028112/-DCSUPPLEMENTAL>
6. A. Rai, O. Nunn, On the impact of increasing penetration of variable renewables on electricity spot price extremes in Australia. *Econom. Anal. Policy* (2020). <https://doi.org/10.1016/j.eap.2020.06.001>
7. B.P. Heard, B.W. Brook, T.M.L. Wigley, C.J.A. Bradshaw, Burden of proof: a comprehensive review of the feasibility of 100% renewable-electricity systems. *Renew. Sustain. Energy Rev.* **76**, 1122–1133 (2017). <https://doi.org/10.1016/J.RSER.2017.03.114>
8. T.W. Brown, T. Bischof-Niemz, K. Blok, C. Breyer, H. Lund, B.V. Mathiesen, Response to burden of proof: a comprehensive review of the feasibility of 100% renewable-electricity systems. *Renew. Sustain. Energy Rev.* **92**, 834–847 (2018). <https://doi.org/10.1016/j.rser.2018.04.113>
9. M. Diesendorf, B. Elliston, The feasibility of 100% renewable electricity systems: a response to critics. *Renew. Sustain. Energy Rev.* **93**, 318–330 (2018). <https://doi.org/10.1016/J.RSER.2018.05.042>
10. M. Arbabzadeh, J.X. Johnson, R. De Kleine, G.A. Keoleian, Vanadium redox flow batteries to reach greenhouse gas emissions targets in an off-grid configuration. *Appl. Energy* **146**, 397–408 (2015). <https://doi.org/10.1016/j.apenergy.2015.02.005>
11. J. Ahmad, M. Imran, A. Khalid, W. Iqbal, S.R. Ashraf, M. Adnan, S.F. Ali, K.S. Khokhar, Techno economic analysis of a wind-photovoltaic-biomass hybrid renewable energy system for rural electrification: a case study of Kallar Kahar. *Energy* **148**, 208–234 (2018). <https://doi.org/10.1016/J.ENERGY.2018.01.133>
12. Lazard: Lazard's levelized cost of storage analysis-version 5.0 (2019) <https://www.lazard.com/media/451087/lazards-levelized-cost-of-storage-version-50-vf.pdf>. Accessed 27 Sept 2020
13. V. Jülch, Comparison of electricity storage options using levelized cost of storage (LCOS) method. *Appl. Energy* **183**, 1594–1606 (2016). <https://doi.org/10.1016/j.apenergy.2016.08.165>
14. P. Denholm, D.J. Arent, S.F. Baldwin, D.E. Bilello, G.L. Brinkman, J.M. Cochran, W.J. Cole, B. Frew, V. Gevorgian, J. Heeter, B.M.S. Hodge, B. Kroposki, T. Mai, M.J. O'Malley, B. Palmintier, D. Steinberg, Y. Zhang, The challenges of achieving a 100% renewable electricity system in the United States. *Joule* **5**(6), 1331–1352 (2021). <https://doi.org/10.1016/j.joule.2021.03.028>
15. K.E. Rodby, T.J. Carney, Y. Ashraf Gandomi, J.L. Barton, R.M. Darling, F.R. Brushett, Assessing the levelized cost of vanadium redox flow batteries with capacity fade and rebalancing. *J. Power Sources* (2020). <https://doi.org/10.1016/j.jpowsour.2020.227958>
16. J. Schmalstieg, S. Käbitz, M. Ecker, D.U. Sauer, A holistic aging model for Li(NiMnCo)O₂ based 18650 lithium-ion batteries. *J. Power Sources* **257**, 325–334 (2014). <https://doi.org/10.1016/j.jpowsour.2014.02.012>
17. M.B. Roberts, A. Bruce, I. MacGill, Impact of shared battery energy storage systems on photovoltaic self-consumption and electricity bills in apartment buildings. *Appl. Energy* **245**, 78–95 (2019). <https://doi.org/10.1016/J.APENERGY.2019.04.001>
18. S.I. Sun et al., Self-sufficiency ratio: an insufficient metric for domestic PV-battery systems? *Energy Procedia* **151**, 150–157 (2018). <https://doi.org/10.1016/j.egypro.2018.09.040>
19. M. Akbari, P. Asadi, M.K.B. Givi, G. Khodabandehlouie, Artificial neural network and optimization. in *Advances in Friction-Stir Welding and Processing* (Woodhead Publishing, New York, 2014), pp. 543–599. <https://doi.org/10.1533/9780857094551.543>
20. EnerNOC: Open Data (2013). <https://open-enernoc-data.s3.amazonaws.com/anon/index.html>. Accessed 08 Oct 2021
21. SolarStrap: Photos. <https://solarstrap.com/commercial-solar-panel/>. Accessed 16 Aug 2021
22. European Commission: Photovoltaic Geographical Information System (PVGIS). https://re.jrc.ec.europa.eu/pvg_tools/en/tools.html. Accessed 11 Aug 2021
23. W.E. Hart, C.D. Laird, J.-P. Watson, D.L. Woodruff, G.A. Hackebeil, B.L. Nicholson, J.D. Sirola, *Pyomo—Optimization Modeling in Python*, 2nd edn. Springer Optimization and Its Applications, vol. 67. (Springer, New York, 2017). <https://doi.org/10.1007/978-3-319-58821-6>
24. Gurobi Optimization inc., *Mathematical Programming Solver*. <http://www.gurobi.com/products/gurobi-optimizer>. Accessed 24 Feb 2022
25. D.C. Jordan, S.R. Kurtz, Photovoltaic degradation rates—an analytical review. *Prog. Photovolt. Res. Appl.* **21**(1), 12–29 (2013). <https://doi.org/10.1002/pip.1182>
26. E1049-85, Standard Practices for Cycle Counting in Fatigue Analysis. 85(Reapproved): 1–10 (1997)
27. V. Viswanathan, A. Crawford, D. Stephenson, S. Kim, W. Wang, B. Li, G. Coffey, E. Thomsen, G. Graff, P. Balducci, M. Kintner-Meyer, V. Sprenkle, Cost and performance model for redox flow batteries. *J. Power Sources* (2014). <https://doi.org/10.1016/j.jpowsour.2012.12.023>
28. D. Reed, E. Thomsen, B. Li, W. Wang, Z. Nie, B. Koepfel, J. Kizewski, V. Sprenkle, Stack developments in a kW class all vanadium mixed acid redox flow battery at the Pacific Northwest National Laboratory. *J. Electrochem. Soc.* **163**(1), 5211–5219 (2016). <https://doi.org/10.1149/2.0281601jes>
29. Live Vanadium Price, News and Articles. <https://www.vanadiumprice.com/>. Accessed 23 Aug 2018
30. D. Roberts, S. Brown, DC to turnkey: an analysis of the balance of costs for behind the meter BESS at commercial/industrial sites. *Energy Rep.* **7**, 20–23 (2021). <https://doi.org/10.1016/j.egy.2021.02.060>
31. K. Mongird, V. Fotedar, V. Viswanathan, V. Koritarov, P. Balducci, B. Hadjerioua, J. Alam, Energy storage technology and cost characterization report. Technical Report PNNL-28866, Pacific Northwest National Laboratory (2019)
32. R. Fu, D. Feldman, R. Margolis, M. Woodhouse, K. Ardani, R. Fu, D. Feldman, R. Margolis, M. Woodhouse, K. Ardani, U.S. solar photovoltaic system and energy storage cost benchmark: Q1 2020. Technical report, NREL (2021)
33. US Department of Energy: Guide to the federal investment tax credit for commercial solar photovoltaics. https://www.energy.gov/sites/prod/files/2020/01/f70/Guide_to_the_Federal_Investment_Tax_Credit_for_Commercial_Solar_PV.pdf. Accessed 30 Aug 2021
34. W. Cole, A.W. Frazier, W. Cole, A.W. Frazier, Cost projections for utility-scale battery storage. Technical Report June, NREL (2019)

35. E. Minear, Energy storage technology and cost assessment: executive summary (2018). <https://www.epri.com/#/pages/product/000000003002013958/?lang=en-US>. Accessed 27 Sept 2020
36. G. Zhang, L. Cao, S. Ge, C.-Y. Wang, C.E. Shaffer, C.D. Rahn, In situ measurement of radial temperature distributions in cylindrical Li-ion cells. *J. Electrochem. Soc.* **161**(10), 1499–1507 (2014). <https://doi.org/10.1149/2.0051410jes>
37. J.M. Reniers, G. Mulder, S. Ober-Blöbaum, D.A. Howey, Improving optimal control of grid-connected lithium-ion batteries through more accurate battery and degradation modelling. *J. Power Sources* **379**, 91–102 (2018). <https://doi.org/10.1016/J.JPOWSOUR.2018.01.004>
38. W.M. Dose, C. Xu, C.P. Grey, M.F.L. De Volder, Effect of anode slippage on cathode cutoff potential and degradation mechanisms in Ni-rich Li-ion batteries. *Cell Rep. Phys. Sci.* (2020). <https://doi.org/10.1016/j.xcrp.2020.100253>